

Effects of driving laser jitter on the attosecond streaking measurement

Shiyang Zhong,¹ Xinkui He,^{1,2} Peng Ye,¹ Minjie Zhan,¹ Hao Teng¹ and Zhiyi Wei^{1,*}

¹Beijing National Laboratory for Condensed Matter Physics, Institute of Physics, Chinese Academy of Sciences, Beijing, 100190, China

²xinkuihe@iphy.ac.cn

zywei@iphy.ac.cn

Abstract: Driving laser jitter is one of the main factors affecting the attosecond streaking measurement. The effect of carrier-envelope phase (CEP) jitter and the pulse energy jitter on the attosecond pulse characterization is studied in this paper. We have theoretically calculated and experimentally confirmed that CEP jitter could result in a symmetry trace in the streaking spectrogram, while the intensity jitter could result in a slight shift and broadening of the trace. Both of them can lead to an underestimate of the retrieved attosecond pulse duration.

©2013 Optical Society of America

OCIS codes: (320.7100) Ultrafast measurements; (140.7240) UV, EUV, and X-ray lasers.

References and links

1. M. Drescher, M. Hentschel, R. Kienberger, M. Uiberacker, V. Yakovlev, A. Scrinzi, T. Westerwalbesloh, U. Kleineberg, U. Heinzmann, and F. Krausz, "Time-resolved atomic inner-shell spectroscopy," *Nature* **419**(6909), 803–807 (2002).
2. R. Kienberger, E. Goulielmakis, M. Uiberacker, A. Baltuska, V. Yakovlev, F. Bammer, A. Scrinzi, T. Westerwalbesloh, U. Kleineberg, U. Heinzmann, M. Drescher, and F. Krausz, "Atomic transient recorder," *Nature* **427**(6977), 817–821 (2004).
3. A. L. Cavalieri, N. Müller, T. Uphues, V. S. Yakovlev, A. Baltuska, B. Horvath, B. Schmidt, L. Blümel, R. Holzwarth, S. Hendel, M. Drescher, U. Kleineberg, P. M. Echenique, R. Kienberger, F. Krausz, and U. Heinzmann, "Attosecond spectroscopy in condensed matter," *Nature* **449**(7165), 1029–1032 (2007).
4. P. Eckle, A. N. Pfeiffer, C. Cirelli, A. Staudte, R. Dörner, H. G. Müller, M. Büttiker, and U. Keller, "Attosecond ionization and tunneling delay time measurements in helium," *Science* **322**(5907), 1525–1529 (2008).
5. A. Schiffrin, T. Paasch-Colberg, N. Karpowicz, V. Apalkov, D. Gerster, S. Mühlbrandt, M. Korbman, J. Reichert, M. Schultze, S. Holzner, J. V. Barth, R. Kienberger, R. Ernstorfer, V. S. Yakovlev, M. I. Stockman, and F. Krausz, "Optical-field-induced current in dielectrics," *Nature* **493**(7430), 70–74 (2012).
6. E. Goulielmakis, M. Schultze, M. Hofstetter, V. S. Yakovlev, J. Gagnon, M. Uiberacker, A. L. Aquila, E. M. Gullikson, D. T. Attwood, R. Kienberger, F. Krausz, and U. Kleineberg, "Single-cycle nonlinear optics," *Science* **320**(5883), 1614–1617 (2008).
7. G. Sansone, E. Benedetti, F. Calegari, C. Vozzi, L. Avaldi, R. Flammini, L. Poletto, P. Villoresi, C. Altucci, R. Velotta, S. Stagira, S. De Silvestri, and M. Nisoli, "Isolated single-cycle attosecond pulses," *Science* **314**(5798), 443–446 (2006).
8. X. Feng, S. Gilbertson, H. Mashiko, H. Wang, S. D. Khan, M. Chini, Y. Wu, K. Zhao, and Z. Chang, "Generation of isolated attosecond pulses with 20 to 28 femtosecond lasers," *Phys. Rev. Lett.* **103**(18), 183901 (2009).
9. J. Itatani, F. Quéré, G. L. Yudin, M. Y. Ivanov, F. Krausz, and P. B. Corkum, "Attosecond streak camera," *Phys. Rev. Lett.* **88**(17), 173903 (2002).
10. Y. Mairesse and F. Quéré, "Frequency-resolved optical gating for complete reconstruction of attosecond bursts," *Phys. Rev. A* **71**(1), 011401 (2005).
11. J. Gagnon, E. Goulielmakis, and V. S. Yakovlev, "The accurate FROG characterization of attosecond pulses from streaking measurements," *Appl. Phys. B* **92**(1), 25–32 (2008).
12. K. Zhao, Q. Zhang, M. Chini, Y. Wu, X. Wang, and Z. Chang, "Tailoring a 67 attosecond pulse through advantageous phase-mismatch," *Opt. Lett.* **37**(18), 3891–3893 (2012).
13. J. Gagnon and V. S. Yakovlev, "The robustness of attosecond streaking measurements," *Opt. Express* **17**(20), 17678–17693 (2009).
14. H. Wang, M. Chini, S. D. Khan, S. Chen, S. Gilbertson, X. Feng, H. Mashiko, and Z. Chang, "Practical issues of retrieving isolated attosecond pulses," *J. Phys. B* **42**(13), 134007 (2009).
15. P. B. Corkum, "Plasma perspective on strong field multiphoton ionization," *Phys. Rev. Lett.* **71**(13), 1994–1997 (1993).
16. M. Lewenstein, P. Balcou, M. Y. Ivanov, A. L'Huillier, and P. B. Corkum, "Theory of high-harmonic generation by low-frequency laser fields," *Phys. Rev. A* **49**(3), 2117–2132 (1994).

17. M. Lewenstein, P. Salières, and A. L'Huillier, "Phase of the atomic polarization in high-order harmonic generation," *Phys. Rev. A* **52**(6), 4747–4754 (1995).
18. M. Chini, S. Gilbertson, S. D. Khan, and Z. Chang, "Characterizing ultrabroadband attosecond lasers," *Opt. Express* **18**(12), 13006–13016 (2010).
19. E. Goulielmakis, "Complete characterization of light waves using attosecond pulses," *Max-Planck-Inst. für Quantenoptik*, 70–72 (2005).

1. Introduction

Recent development in attosecond pulse generation has provided us a new tool for probing or controlling the atomic-scale electron motion in unprecedented time resolution [1–5]. Isolated attosecond pulse rather than attosecond pulse train is needed for attosecond pump and probe experiment. Up to now, isolated attosecond pulses can be generated by amplitude gating [6], polarization gating [7], and generalized double optical gating (GDOG) [8]. The limitation of low flux makes it a challenging task for characterizing these extreme ultraviolet (XUV) pulses. The characterization is realized by the attosecond streaking technique [9]. In this technique, an electron wave packet is ionized by the attosecond XUV pulse in the presence of a NIR laser pulse. The photoelectron momentum is measured as a function of delay between the XUV and NIR pulses. Furthermore, an algorithm based on frequency-resolved optical gating for complete reconstruction of attosecond bursts (FROG-CRAB) is employed for retrieving the temporal amplitude and phase of both the XUV and NIR pulses from the measured spectrogram [10,11]. Isolated attosecond pulses with duration of less than 100 as were successfully retrieved with this technique [6,12].

Some practical factors in the streaking experiment may affect the accuracy of the characterization. Several factors including photoelectron count rate, streaking intensity, time delay jitter and uncertainties of central energy, bandwidth of the wave packet were studied in previous works [13,14]. These results demonstrated the robustness of the reconstruction against experimental limitations. Some factors such as the fluctuations in intensity and CEP of the NIR laser pulse could influence the high-order harmonics generation (HHG) process as well as the streaking measurements, but the effects on the HHG process were not taken into consideration in the works mentioned above. The calculation of the HHG process based on strong field approximation (SFA), and the streaking process based on the Least-Squares Generalized Projections Algorithm (LSGPA) [11] are combined in this work in order to correctly estimate the effects of intensity jitter and CEP jitter of the NIR pulse on the attosecond streaking measurements.

2. Basic model

When an intense ultrashort laser pulse is focused to a rare gas jet, high-order harmonics of the laser pulse is generated. The mechanism of HHG can be well described with the famous three-step model [15], in which a valence electron is tunneling ionized from the atom, accelerated in the laser field and then recombines with the parent nuclei to emit high energy photon. A quantum version of the three-step model has been developed [16,17] based on the strong field approximation. It is assumed that only the ground state and the continuum states are engaged in this theory. The Coulomb field for the electron in the continuum is also neglected since it is much weaker compared with the intense laser field. The dipole moment of the electron producing the HHG radiation is given by [16]

$$r(t) = i \int_{-\infty}^t dt' \int d^3 p E(t') d^* (p - A_L(t)) d (p - A_L(t')) \exp(-iS(p, t', t)) + c.c., \quad (1)$$

$$S(p, t', t) = \int_{t'}^t dt'' \left(\frac{(p - A_L(t''))^2}{2} + I_p \right). \quad (2)$$

Where p is the momentum of the free electron, $E(t)$ is the electric field of the NIR laser, $d(p)$ is the dipole transition matrix element between the ground state and continuum states, $A_L(t)$ is the vector potential of the NIR laser, t' and t are the ionization and re-collision time respectively. $S(p, t', t)$ is the classical action term, and I_p is the ionization potential of the

atom. The HHG spectrum can be calculated from the Fourier transform of the dipole acceleration. Amplitude gating approach is simulated in this work. A spectral filter is set in order to simulate the spectrum selection of the Mo/Si mirror, which is used to focus the XUV beam in the streaking experiment. Only the single atom response is concerned in our calculation, which should be enough for the amplitude gating experiment with thin rare gas medium.

In the streaking experiment, electrons bounded by coulomb potential I_p are ionized by the XUV pulse. The photoelectron wave packet is a replica of the XUV pulse to be measured. The NIR field will introduce a momentum shift proportional to the vector potential to the free electrons. The modulated momentum distribution is measured as a function of the delay τ between the XUV and NIR pulses. The temporal information of the XUV and NIR pulses is encoded in the measured spectrogram which can be given in atomic units by [11]

$$S(p, \tau) = \left| \int_{-\infty}^{\infty} E_X(t) d(p + A_L(t + \tau)) \exp(-i\varphi(p, t + \tau)) \exp(i(\frac{p^2}{2} - \Omega_X + I_p)t) dt \right|^2, \quad (3)$$

$$\varphi(p, t) = \int_t^{\infty} \left(p A_L(t') + \frac{1}{2} A_L^2(t') \right) dt'. \quad (4)$$

Where $E_X(t)$ is the complex envelope of the XUV pulse, $\varphi(p, t)$ is the phase shift induced by the NIR pulse, Ω_X is the central energy of the XUV pulse. The XUV and NIR fields are assumed to be linearly polarized in the same direction which is also set to be the observation direction.

However, we still have to make a couple of approximations to change the form of $S(p, \tau)$ given in (3) into a standard FROG spectrogram. First, the transition dipole matrix element $d(p + A_L(t + \tau))$ is assumed to be constant since the photoionization cross-section of certain gases is almost constant of the bandwidth of the spectral filtered attosecond pulses. Second, momentum p is substituted with the central momentum of the streaked electrons p_C . The second approximation is also named the central momentum approximation which is a main limitation while dealing with a broadband attosecond pulse [18]. The streaking spectrogram can be finally expressed as

$$S(p, \tau) = \left| \int_{-\infty}^{\infty} E_X(t) G(t + \tau) \exp(i(\frac{p^2}{2} - \Omega_X + I_p)t) dt \right|^2, \quad (5)$$

$$G(t + \tau) = \exp \left[-i \int_t^{\infty} \left(p_C A_L(t') + \frac{1}{2} A_L^2(t') \right) dt' \right]. \quad (6)$$

The retrieval of the XUV and NIR fields from a FROG-CRAB trace is done using LSGPA. This algorithm introduces an iterative procedure. A complex spectrogram S is firstly computed via (5) from an initial guess of the pair $\{E_X(t), G(t)\}$. Then its modulus is substituted by the measured trace to get a new spectrogram S' . An optimal pair of $\{E'_X(t), G'(t)\}$ can be calculated from S' . The newly obtained pair can be used as the guess for the next iteration. Such iterations are repeated until it reaches convergence and retrieve the XUV and NIR pulses from the final pair.

3. CEP jitter

The CEP stability of the NIR laser is one of the crucial factors for generating and characterizing isolated attosecond pulses in amplitude gating method since a pulse duration of less than 2 optical cycles is required. A CEP shift in driving laser will result in a change in HHG spectrum which affects the number and relative amplitude of the attosecond bursts selected from the spectral filter, and it can also affect the following streaking measurements

by introducing a different momentum shift in the measured trace. Our simulation is designed for studying these effects because of their potential to damage the reconstruction.

In this simulation, the NIR pulse has a Gaussian shape expressed by

$$E(t) = E_0 \exp(-2 \log(2) t^2 / T^2) \cos(\omega t + \Phi_{CE}) \quad (7)$$

Here, T is the pulse duration in FWHM, E_0 is the amplitude of the streaking field, ω is the angular frequency, and Φ_{CE} is the CEP of the pulse. The NIR pulse is assumed to be 4 fs centered at 750 nm with a peak intensity of $3 \times 10^{14} W/cm^2$ in the HHG process and $1 \times 10^{12} W/cm^2$ in the streaking process. A Gaussian-shaped spectral filter is set to be centered at 80 eV with a bandwidth of 16 eV to select spectrum in the cut-off region. The attosecond bursts sent to the streaking process are the inverse Fourier transform of the filtered spectrum. The gas used in the HHG and streaking experiment is set to be neon with a ionization potential of 21.56 eV. Thus the ionized electron wave packet has a kinetic energy centered at ~ 58 eV. The time delay step is chosen to be 167 as to simulate the practical experimental parameter. A spectrogram with jitter noise is an accumulation of spectrums shot by shot. Each spectrum is computed via (5) at a certain delay time τ , and the CEP fluctuation expressed by its root mean square (RMS) with an average of 0.

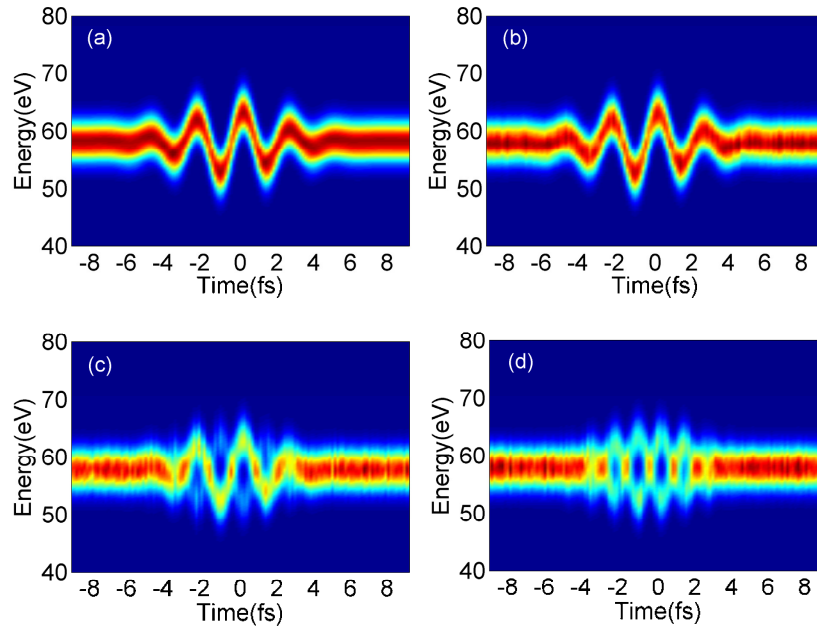


Fig. 1. Simulated spectrograms with (a) no CEP jitter. (b) a CEP jitter RMS of 0.6 rad. (c) RMS of 1.4 rad. (d) a random CEP jitter

The calculated CRAB traces with noise are smeared compared to the noise free one as shown in Fig. 1. An opposite trace becomes obvious when the CEP jitter RMS is more than 1.4 rad, and it becomes symmetrical to the noise free trace when the CEP is random as shown in Fig. 1(d). This pattern is in good agreement with the experimentally obtained trace with random phase [19] and will be referred to as “symmetry trace” in this article. These results demonstrate the crucial role that NIR waveform plays in attosecond generation and characterization. A cosine waveform or an anti-cosine waveform leads to only one main attosecond burst after the spectral filter while a sine waveform leads to two attosecond bursts with equal amplitude separated by half period of the driving laser field. Any intermediate waveform results in two bursts with different amplitudes. The attosecond bursts from the

cosine and anti-cosine waveform have almost the same amplitude with phase difference of π , hence the streaked electrons received similar modulation but in opposite directions. The spectrogram from the sine waveform will show an interference pattern, but it contributes less since the two bursts are much weaker than the one in a cosine waveform case because of the nonlinear relationship between the intensity of NIR pulse and the generated XUV pulse. The intermediate waveform contributes an intermediate pattern, but only those who produce a dominate burst and a weak satellite burst contributes more. That's the reason why the symmetry counterpart appears only when the CEP jitter reaches the anti-cosine waveform, i.e. $\Phi_{CE} = \pm \pi$, and the spectrogram is not much smeared by the two-bursts interference pattern.

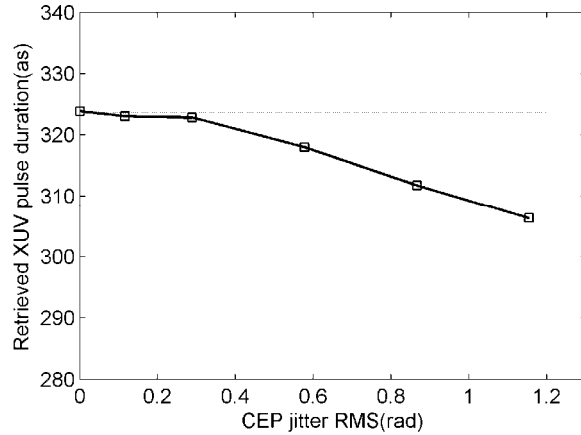


Fig. 2. Retrieved XUV pulse duration as a function of the CEP jitter RMS.

Figure 2 shows the retrieved pulse duration as a function of CEP jitter RMS after 1000 iterations. The retrieved duration deviates from the initial duration only when the RMS is more than 0.4 rad which roughly corresponds to a CEP jitter from $-\pi/4$ to $\pi/4$. These results indicate a general underestimate of the duration since the noise tends to broaden the trace, but it will not be a severe problem since the CEP fluctuation of a state-of-the-art CEP stabilized laser could be controlled in 200 mrad. But in case that only the CEP of the oscillator is locked, the jitter induced by the amplifier may affect the result, and the retrieval algorithm will not convergent when the RMS is more than 1.2 rad because of the smearing of the symmetry trace.

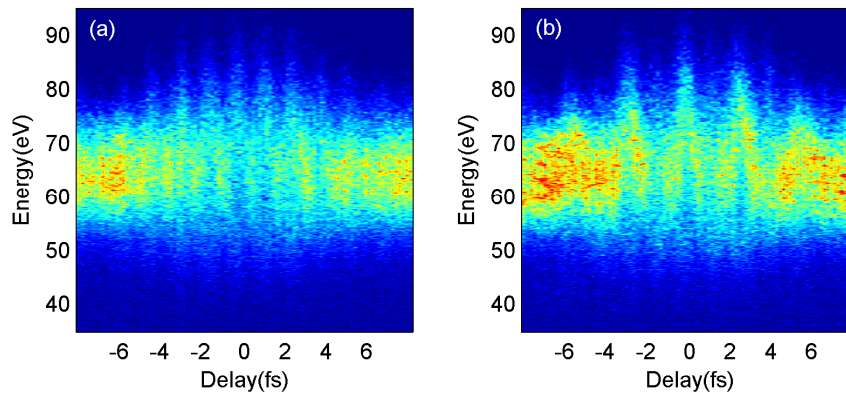


Fig. 3. Experimental spectrogram on condition that (a) the CEP of the oscillator and amplifier is unlocked. (b) only the CEP of the amplifier is unlocked.

The simulation is confirmed by the experiment carried out in our lab as shown in Fig. 3. A kHz 5-fs laser with a pulse energy of 0.4 mJ was used as the driving laser in the experiment. The attosecond pulse was generated by focusing the driving laser into a 1mm neon gas jet and selected by a Mo/Si-coated mirror with max reflectivity of 8% at 83 eV. The selected pulse was further measured by the streaking camera. The spectrogram recorded in a random CEP case is shown in Fig. 3(a), the peaks are separated by half an optical cycle instead of one cycle just as Fig. 1(d) indicates. The symmetry is not so perfect as in the simulation because of the imperfections of other experimental factors. The streaking spectrogram recorded with only oscillator CEP locked case is shown in Fig. 3(b) which is similar to the result in Fig. 1(c). The symmetry trace appears but is quite weak compared to the main trace. The slow fluctuation after the amplifier in case that only oscillator CEP is locked oscillates much slower than a fast fluctuation. The slow fluctuation in a 10 second acquisition time for one step of time delay is generally small enough to recognize a main trace.

4. Intensity jitter

The intensity jitter of the driving laser is another key factor that may limit the accuracy of the measurement. The fluctuation in laser intensity will change the amplitude and central energy of the generated attosecond bursts, thus it introduces smearing and shift in the spectrogram.

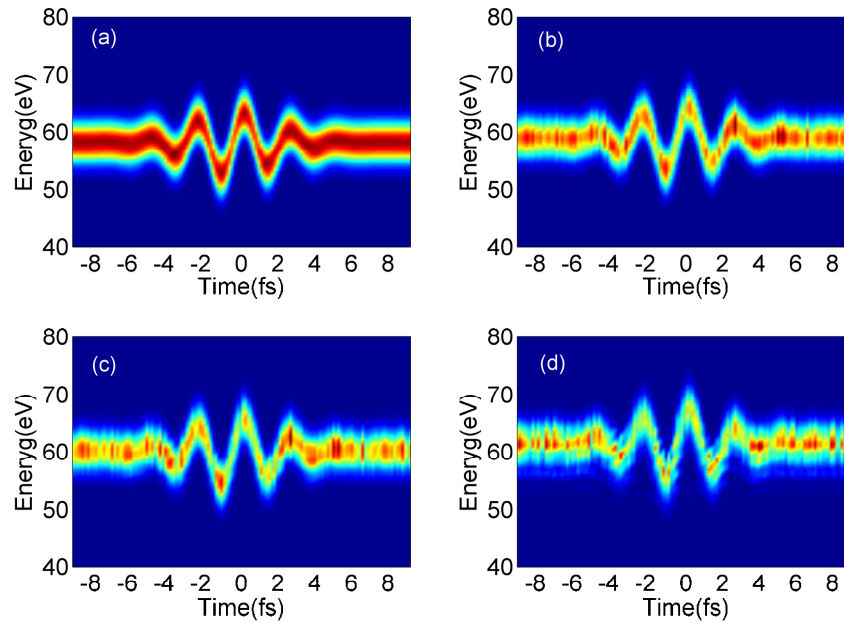


Fig. 4. Simulated spectrogram with (a) no intensity jitter. (b) STD of 5.8%. (c) STD of 11.6%. (d) STD of 17.3%.

In order to study this effect on the attosecond pulse reconstruction, a similar simulation is done with the same parameters in the previous part except that the CEP of the NIR pulse is fixed and its amplitude fluctuates from shot to shot. The fluctuation is expressed by the standard deviation (STD) in atomic unit. The smearing appears even in a small jitter and tends to be more severe with the jitter grows as Fig. 4 shows. The central energy shifts from 58 eV to 61 eV at a STD of 17.3%. The fluctuation in NIR pulse intensity results in a shift in central energy of the attosecond pulse that broadens the spectrum. But the XUV pulse generated from a stronger NIR pulse usually has larger amplitude that makes it contribute more in the spectrogram, so the trace tends to shift to a higher energy rather than a broadening in both

directions. The broadening effect will be strong only if the energy shift is large enough as the low energy shadow part implies in Fig. 4(d).

The reconstruction results are shown in Fig. 5. The retrieved duration deviates very slightly even in a STD of 11.6%, and an underestimate of 10% is induced by a STD of 17.3% because of the broadening. It indicates a good robustness against intensity jitter since generally the intensity fluctuation of a kHz laser should be better than 3%.

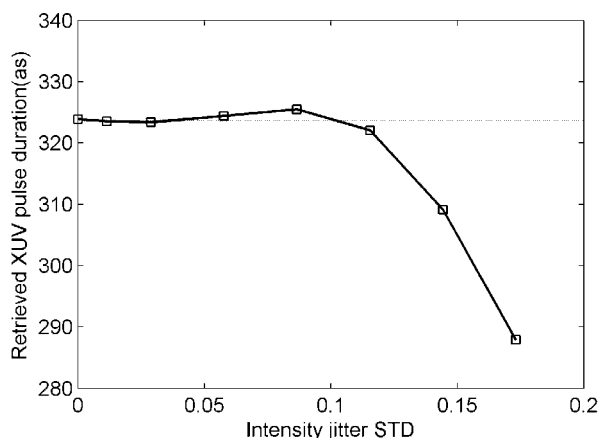


Fig. 5. Retrieved XUV pulse duration as a function of the intensity jitter STD.

5. Conclusion

In this work, we studied the effect of CEP jitter and intensity jitter of the driving laser on the attosecond pulse characterization using streaking technique. These two factors involve both the HHG process and the streaking process. We have shown that the CEP jitter could result in a symmetry trace in the spectrogram, which is confirmed by our experiment result. The intensity jitter can result in a slight shift and broadening of the trace. Both of them can lead to an underestimate of the retrieved duration. Our results are helpful for judging the origin of some noises in the experimentally measured CRAB trace that makes it possible to optimize the experiment parameters.

Acknowledgments

We thank the helpful discussions by Dr Wei Zhang and Dr Lifeng Wang, this work is partly supported by the National Key Basic Research Program of China under Grant No.2013CB922402 and the International Joint Research Programme of National Natural Science Foundation of China under grant No: 61210017. As well as the Instrument Developing Project of the Chinese Academy of Sciences, Grant No. 2010004